Response to referee comments on "An Integrated Synchronous Online Analyzer for Gaseous and Particulate Reactive Oxygen Species (ROS): Development, Characterization and Field Observations"

We sincerely thank the editors and the reviewers for their valuable comments and constructive suggestions on our manuscript. These comments have been very helpful in improving the quality, clarity, and scientific rigor of the manuscript. We have carefully considered all comments and revised the manuscript accordingly. The main revisions and our point-by-point responses to the reviewer's comments are provided below. The reviewer's comments are shown in black, our responses in **blue**, and the text added to the revised manuscript in ***blue italics***.

Response to Anonymous Referee #1:

This manuscript presents the development and application of an integrated online system for simultaneous measurements of gaseous and particulate reactive oxygen species (ROS). As ROS is a key driver of atmospheric oxidative potential and associated health impacts, the ability to measure gas-phase and particle-phase ROS synchronously is valuable for improving our understanding of atmospheric chemistry and exposure pathways. Overall, this work is within the scope of AMT, the developed instrument is well-characterized, and the four-season field observation validates the robust application of the instrument. However, several issues need to be addressed before publication.

Comment 1: The paper would be strengthened by a direct comparison table of the present instrument vs. earlier online ROS analyzers (e.g., the instrument by Huang et al., AE, 2016; King and Weber, AMT, 2013). Compare the key parameters: time resolution, LOD for gas and particle phase, reagent consumption, portability, and major artifacts. Also, clarify how the present system differs from the earlier instruments.

Response 1: We are very thankful for the reviewer's comment. In response to this comment, we have added Sect. **3.2.5 Performance comparison** and included a new comparison table (**Table 3**) summarizing representative DCFH/HRP-based online atmospheric ROS analyzers, including those reported by King and Weber (2013), Huang et al. (2016), Wragg et al. (2016), Zhou et al. (2018), and

Liu et al. (2023) in the revised manuscript. We further clarified that the main advance of the present analyzer is its independent dual-channel phase-resolved configuration. Specifically, ROS_g is collected using a low-holdup glass spiral absorber, while ROS_p is measured through a separate WAD-assisted, ambient-temperature spray-growth collection channel. This design allows direct and synchronous quantification of ROS_g and ROS_p without relying on difference-based calculation, thereby reducing uncertainty propagation associated with subtraction. In addition, the ambient-temperature particle collection helps reduce potential losses of labile ROS_p. Together with compact LED-PMT fluorescence detection, the present analyzer provides improved phase resolution, rapid response, and field-deployable operational integration. We also noted that, as with other DCFH/HRP-based systems, the measured concentrations should be interpreted as operational H_2O_2-equivalent ROS rather than molecule-specific ROS.

Revision in the manuscript:

3.2.5 Performance comparison (line 313-334)

Table 3 summarizes the evolution of representative DCFH/HRP-based online atmospheric ROS analyzers in terms of target phase, sampling strategy, response time, detection limit, reagent use, and major constraints. The semi-continuous method of King and Weber (2013) enabled online ROS measurements with a 10.5 min cycle, but ROS_p was obtained by subtracting ROS_g from total ROS, making the result sensitive to uncertainty propagation when particle-phase signals were near the detection limit. Huang et al. (2016) developed the GAC-ROS system for simultaneous ROS_g and ROS_p measurements; however, the relatively complex gas/aerosol collection and liquid-handling configuration limited further simplification and integration for field deployment. OPROSI reported by Wragg et al. (2016) improved portability and achieved a time resolution of ≤12 min, but it targeted ROS_p only and therefore could not resolve synchronous ROS_p variations. Zhou et al. (2018) achieved an approximately 8 min fluorescence response and improved reagent handling and interference characterization, yet the system remained particle-focused and showed notable sensitivity variability. Liu et al. (2023) reduced offline sampling losses and provided online ROS_p monitoring with a 20 min resolution, but ROS_p was still calculated from alternating total and gas-phase measurements.

The present analyzer was developed to improve phase resolution, response speed, and operational integration simultaneously. By coupling a low-holdup glass spiral absorber for ROS_g with a separate WAD-assisted, ambient-temperature spray growth collector for ROS_p, the system directly quantifies both phases without difference-based calculation. This design reduces uncertainty propagation, improves the ability to capture rapid gas-particle variations, and minimizes potential collection losses of labile particulate ROS. Together with compact LED-PMT fluorescence detection, the analyzer achieved a 7 min response time, low detection limits for both phases, and stable long-term operation, demonstrating its suitability for synchronized field measurements of atmospheric ROS. As with other DCFH/HRP-based systems, the reported concentrations should be interpreted as operational H_2O_2-equivalent ROS rather than molecule-specific ROS.

Table 3 Technical comparison of representative DCFH/HRP-based online atmospheric ROS analyzers

Reference	*Phase*	*Time resolution*	*LOD*	*DCFH/HRP consumption*	*Key feature/limitation*
This study	*ROS_g/ROS_p*	*7 min*	*ROS_g: 0.07 ppbv ROS_p: 0.007 μg m^{-3}*	*0.60 mL min^{-1}*	*Direct ROS_g/ROS_p quantification; Operational H_2O_2-equivalent ROS only*
King and Weber (2013)	*ROS_p*	*10.5 min*	*0.005 μg m^{-3}*	*0.86 mL min^{-1}*	*Semi-continuous online measurement; Subtraction-derived ROS_p*
Huang et al. (2016)	*ROS_g/ROS_p*	*/*	*ROS_g: 0.004 ppbv ROS_p: 0.004 μg m^{-3}*	*/*	*Simultaneous dual-phase measurement; Complex liquid handling*
Wragg et al. (2016)	*ROS_p*	*12 min*	*0.14 μg m^{-3}*	*2.0 mL min^{-1}*	*Portable ROS_p measurement; No gas-phase channel*
Zhou et al. (2018)	*ROS_p*	*8 min*	*0.068 μg m^{-3}*	*0.40 mL min^{-1}*	*Rapid ROS_p response; Sensitivity variability*
Liu et al. (2023)	*ROS_p*	*20 min*	*0.065 μg m^{-3}*	*0.20 mL min^{-1}*	*Online ROS_p monitoring; Alternating measurement modes*

Comment 2: The authors did interference assessments with individual species. However, in the real atmosphere, these soluble species coexist, and do the authors also test with the mixture of all these soluble species (i.e., O_3, NO_x, SO_2, and transition metals)?

Response 2: We indeed appreciate the reviewer's insight into the study. We agree that coexisting soluble species may produce combined interferences that cannot be fully evaluated from individual tests alone. To address this concern, we added direct mixed-interferent experiments under the same DCFH-HRP

conditions used in the analyzer.

Specifically, a 3 μg L^{-1} H_2O_2 solution was used as the reference matrix, and SO_2, NO, Fe^{2+}, and their mixtures were tested against the H_2O_2-only control. In addition to the individual tests, two mixed conditions were examined: M1, an environmentally representative mixed condition composed of S2, N2, and F2, and M2, a high-level sensitivity condition composed of S3, N4, and F3. The results are now presented in the newly added Figure 4 and discussed in Sect. **3.3 Interference assessment**.

The mixed-interferent tests showed that the combined effect was mainly negative and was governed by SO_2 and Fe^{2+}. The total bias was −3.23% under M1 and −11.03% under M2. Based on the calibration conversion used in this study, the M1 bias corresponds to approximately −0.056 ppbv for ROS_g and −0.006 μg m^{-3} for ROS_p, which is close to or below the instrumental detection limits. The M2 bias corresponds to approximately −0.19 ppbv for ROS_g and −0.022 μg m^{-3} for ROS_p and represents a conservative high-level sensitivity scenario. These results indicate that the environmentally representative mixed interference was unlikely to affect the seasonal pattern or pollution-regime interpretation of the field observations.

O_3-related interference was evaluated based on previous DCFH-HRP characterizations and the observed O_3 levels during the field campaign. Earlier studies showed negligible DCFH responses at 60-80 ppbv O_3 and a maximum H_2O_2 quantification error below 0.03 ppbv even at 100 ppbv O_3, whereas positive artifacts became important only under much higher O_3 levels due to secondary oxidant formation. Since the observed O_3 levels in this study were within the ambient-relevant range evaluated in these studies, O_3-related interference was considered minor relative to the direct negative effects of SO_2 and Fe^{2+}.

Revision in the manuscript:

The following text and figure were revised in Sect. 3.3 Interference assessment (line 336-375):

Potential interferences in the DCFH-HRP assay may arise from direct probe oxidation, aqueous consumption of H_2O_2, or side reactions affecting DCF formation. For oxidizing gases, previous studies have shown that O_3 interference is generally weak under ambient-relevant conditions. The dissolved O_3 level estimated at ~40 ppbv is insufficient to produce measurable DCFH-based artifacts, and laboratory tests at 60-80 ppbv O_3 showed negligible responses (Huang et al., 2016; King and Weber, 2013). Field

evaluations further indicated that even 100 ppbv O_3 produced a maximum H_2O_2 quantification error below 0.03 ppbv, whereas positive artifacts became important only under extremely elevated O_3 levels up to several hundred ppbv due to secondary oxidant formation (Lazrus et al., 1986; Montesinos et al., 2015). Since the O_3 levels observed in the present campaign were within the ambient-relevant range evaluated in these studies, O_3-related interference was considered a minor positive artifact in the gas-phase channel.

Reducing gases and soluble transition metals were more directly relevant to potential negative biases in the present DCFH-HRP configuration. NO has been reported to cause only weak H_2O_2 loss, whereas SO_2 can suppress H_2O_2 detection through aqueous S(IV) chemistry with strong dependence on concentration and pH (Hua et al., 2008; Lazrus et al., 1986; Komazaki et al., 2001). Fe^{2+} can also consume H_2O_2 through Fenton-type reactions, while Fe^{3+} shows limited interference under comparable conditions (Kolthoff and Medalia, 1949; Zhou et al., 2018). Therefore, direct laboratory tests were conducted for SO_2, NO, Fe^{2+}, and their mixtures under the same reaction conditions as the analyzer. The interference tests used a 3 μg L^{-1} H_2O_2 standard as the reference solution, and the H_2O_2-only solution was used as the control. The tested atmospheric-equivalent levels included 0.5, 1, 10, and 25 ppbv for SO_2; 10, 25, 50, and 100 ppbv for NO; and 20, 80, 160, and 400 ng m^{-3} for Fe^{2+}. Two mixed conditions were further examined: Mix1, an environmentally representative mixed condition composed of 1 ppbv SO_2, 25 ppbv NO, and 80 ng m^{-3} Fe^{2+}, and Mix2, a high-level sensitivity condition composed of 10 ppbv SO_2, 100 ppbv NO, and 160 ng m^{-3} Fe^{2+}. As shown in Figure 4, NO produced negligible interference across the tested range, with biases from −1.02% to 0.04%. SO_2 showed a clear concentration-dependent negative effect. The biases were minor at 0.5 and 1 ppbv SO_2 (−0.20% and −0.23%) but increased to −10.00% and −29.97% at 10 and 25 ppbv SO_2, respectively, consistent with H_2O_2 consumption by dissolved S(IV). Formaldehyde was not used in the present flow configuration; therefore, SO_2-related effects were retained as a potential negative interference rather than assumed to be chemically suppressed.

Fe^{2+} also caused a systematic negative bias, increasing from −0.05% at 20 ng m^{-3} to −2.73%, −4.69%, and −7.53% at 80, 160, and 400 ng m^{-3}, respectively. This trend agrees with Fe(II)-driven Fenton-type H_2O_2 consumption. The mixed-interferent tests provided a direct estimate of total interference under coexisting soluble species. The total bias was −3.23% for Mix1 and −11.03% for Mix2, indicating that

the combined effect was mainly negative and governed by SO_2 and Fe^{2+}, without evidence of additional synergistic amplification.

Based on the calibration conversion used in this study, the Mix1 bias corresponds to an atmospheric-scale uncertainty of approximately −0.056 ppbv for ROS_g and −0.006 μg m^{-3} for ROS_p, which is below the instrumental detection limits. The Mix2 bias corresponds to approximately −0.19 ppbv for ROS_g and −0.022 μg m^{-3} for ROS_p and represents a conservative high-level sensitivity scenario. Therefore, the quantified interference was unlikely to affect the seasonal pattern or pollution-regime interpretation of the present field observations, although high-SO_2 or Fe-rich environments may lead to underestimation of ROS and should be further evaluated in future applications.

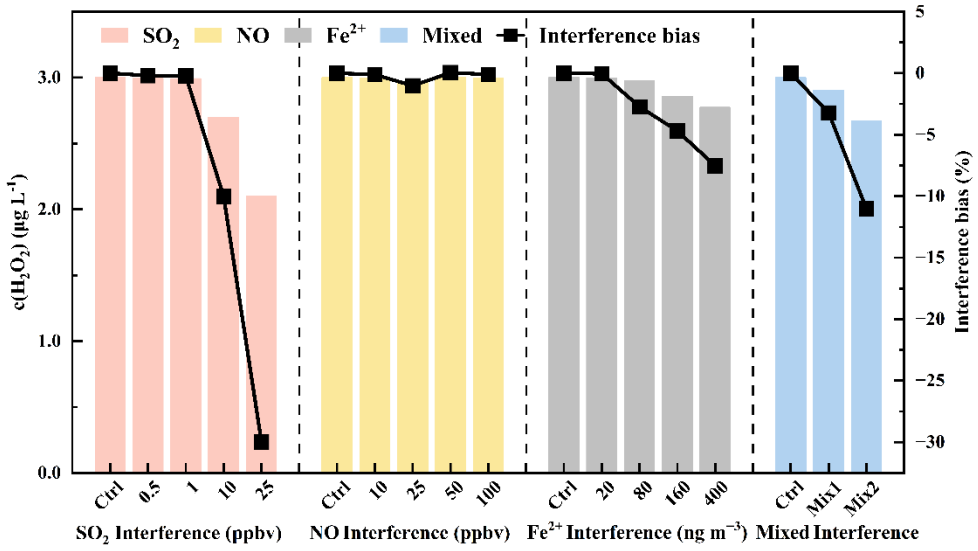

Figure 4. *Effects of SO_2, NO, Fe^{2+}, and mixed interferents on the DCFH-HRP response to 3 μg L^{-1} H_2O_2. SO_2 and NO levels are given in ppbv, and Fe^{2+} levels in ng m^{-3}. Mix1 contains 1 ppbv SO_2, 25 ppbv NO, and 80 ng m^{-3} Fe^{2+}, while Mix2 contains 10 ppbv SO_2, 100 ppbv NO, and 160 ng m^{-3} Fe^{2+}. Bars indicate measured H_2O_2-equivalent concentrations, and black squares indicate interference bias relative to the control.*

The following text was added to Sect. 5 Conclusions (line 591-594):

Direct interference tests showed that NO caused negligible bias, whereas elevated SO_2 and Fe^{2+} could introduce negative interferences. The environmentally representative mixed-interferent condition produced only a small bias close to or below the instrumental detection limits, indicating that the

quantified interference was unlikely to affect the field interpretation. Nevertheless, high-SO_2 or Fe-rich environments may lead to ROS underestimation and should be further evaluated.

Comment 3: All ROS concentrations are expressed as "H_2O_2 equivalents" using H_2O_2 standards. Given that ambient ROS comprises a mixture of peroxides, radicals, and possibly other oxidants, the authors should clarify the sensitivity of the DCFH probe to different types of ROS and discuss the possible limitations of using the DCFH assay.

Response 3: We agree that ambient ROS comprise a chemically diverse mixture and that the DCFH-HRP assay does not respond equally to different ROS species. Therefore, concentrations calibrated with H_2O_2 standards should not be interpreted as molecule-specific or total ROS concentrations.

To address this concern, we have revised the end of Sect. **2.2 Instrument principle** to clarify the chemical sensitivity and operational nature of the DCFH-HRP method. Specifically, we added that previous characterization of DCFH-based atmospheric ROS measurements showed species-dependent responses: peracetic acid produced a fluorescence response close to that of H_2O_2, whereas sterically hindered organic peroxides such as tert-butyl hydroperoxide, benzoyl peroxide, lauroyl peroxide, and 2-butanone peroxide exhibited much lower relative sensitivities (Zhou et al., 2018). This indicates that the DCFH signal depends on the chemical structure, aqueous stability, and reactivity of individual ROS species.

We further clarified that the measured signal represents an operationally defined fraction of water-soluble, DCFH-reactive oxidants rather than the total abundance or molecular composition of atmospheric ROS. Accordingly, the reported ROS_g and ROS_p values are appropriate for internally consistent comparisons of temporal, seasonal, and phase-dependent variations under the same sampling and detection protocol, but should not be used to resolve absolute molecule-specific ROS concentrations.

Revision in the manuscript:

The following text was added to Sect. 2.2 Instrument principle (line 119-126):

It should be noted that the DCFH-HRP assay is not equally sensitive to all ROS species. Previous characterization of DCFH-based atmospheric ROS measurements showed that peracetic acid produced

a response close to that of H_2O_2, whereas sterically hindered organic peroxides, such as tert-butyl hydroperoxide, benzoyl peroxide, lauroyl peroxide, and 2-butanone peroxide, exhibited much lower relative sensitivities (Zhou et al., 2018). Therefore, the measured signal represents an operationally defined fraction of water-soluble, DCFH-reactive oxidants expressed as H_2O_2 equivalents, rather than the total abundance of all atmospheric ROS. Consequently, ROS species with low DCFH-HRP reactivity or limited aqueous stability may contribute less efficiently to the fluorescence signal, resulting in species-dependent response biases.

Comment 4: The ROS_p collection efficiency (91.2%) was derived from recovery experiments with three fractions (chamber liquid, wall rinse, backup filter). Was this efficiency constant over the range of ambient PM loads and compositions? High PM loading might alter wall loss or droplet growth efficiency. Also, please clarify the reproducibility of the efficiency measurement (e.g., triplicate tests) and whether it was rechecked after extended field use.

Response 4: We thank the reviewer for this valuable comment. We agree that the ROS_p collection efficiency should be defined within the operating conditions under which it was determined, rather than treated as a universally constant parameter. To address this concern, we revised Sect. **2.4 Instrument calibration** to clarify the determination, reproducibility, and applicable scope of the collection efficiency.

The recovery experiment was performed in triplicate under actual ambient aerosol sampling conditions during the present field deployment. The recovered material was separated into three fractions: the chamber-collected liquid, the wall-rinse solution, and the downstream backup filter. The mean recovered fractions were 81.72%, 9.46%, and 8.80%, respectively. The wall-rinse and backup-filter fractions were used to evaluate wall deposition and particle breakthrough, respectively. Because only the chamber-collected liquid was continuously introduced into the online detection pathway, this fraction was used as the effective online collection efficiency for ROS_p quantification.

The revised text further clarifies that this value represents an operational mean collection efficiency for the present field deployment, rather than a universally constant efficiency under all aerosol conditions. Potential variations associated with particle loading, hygroscopic growth, aerosol chemical composition, and long-term operation are now acknowledged as factors requiring further evaluation. In addition, a concise statement was added to Sect. **5 Conclusions** to define the applicable scope of the ROS_p collection

efficiency and to indicate that further systematic evaluation is needed in future applications.

Revision in the manuscript:

The following text was added to Sect. 2.4 Instrument calibration (line 212-219):

The recovery experiment was conducted in triplicate under actual ambient aerosol sampling conditions. The mean recovered fractions were 81.72% in the chamber-collected liquid, 9.46% in the wall-rinse solution, and 8.80% on the downstream backup filter. The wall-rinse and backup-filter fractions were used to evaluate wall deposition and particle breakthrough, respectively. Since only the chamber-collected liquid was directly delivered to the second premixing chamber during routine online operation, γ_p = 81.72% was used as the effective online collection efficiency for ROS_p quantification in Eq. (2.4). This value represents an operational mean collection efficiency for the present field deployment. Potential variations associated with particle loading, hygroscopic growth, aerosol chemical composition, and long-term operation should be further evaluated in future applications.

The following text was added to Sect. 5 Conclusions (line 594-597):

In addition, the ROS_p collection efficiency was determined from triplicate recovery experiments under actual ambient aerosol sampling conditions; its potential dependence on particle loading, hygroscopic growth, aerosol chemical composition, and extended field operation should be further evaluated in future applications.

Comment 5: Line 134: "~0.13 s" residence time in the glass spiral absorber. How was this estimated? Provide the calculation or a reference.

Response 5: In response to this comment, we have revised Sect. **2.3.1 Sample collection process** to provide a clearer explanation of the estimated residence time in the glass spiral absorber. The reported value of ~0.13 s is a nominal gas-liquid contact time estimated from the internal volume of the glass spiral coil and the total flow rate through the absorber. Under the stated absorber geometry, the internal coil volume is approximately 2.2 mL. During operation, the gas sampling flow rate was 1.0 L min^{-1}, while the absorbent flow rate was 1.0 mL min^{-1}, yielding an estimated contact time of 0.13 s. Because the liquid flow rate is negligible relative to the gas flow rate, this estimate is mainly controlled by the gas

residence time in the spiral coil.

Revision in the manuscript:

The following text was added to Sect. 2.3.1 Sample collection process (line 140-144):

Surface tension maintains a stable liquid film along the inner wall of the spiral absorber, ensuring continuous gas-liquid contact for ROS_g uptake. Under the present geometry and flow conditions, the internal coil volume was approximately 2.2 mL, corresponding to an estimated gas-liquid contact time of ~0.13 s. Because the absorbent flow rate was negligible relative to the gas flow rate, this estimate was governed primarily by the gas residence time within the spiral coil.

Comment 6: Please provide a brief introduction about the field site used for instrument validation.

Response 6: We are grateful to the reviewer for pointing this out. In response to this comment, we have added a brief description of the field site in Sect. **4.1 Observation methods**, The revised text now specifies that the measurements were conducted at the Peking University Computing Center in Haidian District, northwestern Beijing, which is located in the Zhongguancun urban area. The surrounding urban setting, including educational, commercial, residential, and traffic activities, as well as the influence of local emissions and regional transport, has been described to clarify the atmospheric conditions under which the analyzer was validated.

Revision in the manuscript:

The following text was added to Sect. 4.1 Observation methods (line 378-385):

Field observations of ROS_g and ROS_p were conducted at the Peking University Computing Center in Haidian District, northwestern Beijing, China (39.99 ^{o}N, 116.31 ^{o}E). The site is located in the Zhongguancun area, a densely populated urban district characterized by intensive educational, commercial, residential, and traffic activities. It is therefore affected by mixed urban emissions, including vehicle exhaust, residential and commercial activities, and regional transport from surrounding areas of the North China Plain. These features provide a complex urban atmospheric environment for evaluating the field applicability of the analyzer under seasonally varying photochemical and particulate

pollution conditions. The field campaign covered four seasons: autumn (October 29-November 15, 2024), winter (December 10-31, 2024), spring (April 24-May 15, 2025), and summer (June 13-July 5, 2025).

Comment 7: Line 344, ROS_g and ROS_p have the same seasonal pattern, why "whereas" is in the sentence?

Response 7: We thank the reviewer for pointing this out. We agree that "whereas" was inappropriate in this sentence because ROS_g and ROS_p showed the same seasonal pattern, with both phases reaching their maxima in spring and minima in autumn. We have revised the sentence to avoid implying a contrast between the two phases and to more clearly state their consistent seasonal behavior.

Revision in the manuscript:

The following text was revised in 4.2. Overall variations of ROS and associated atmospheric species (line 399-401):

Notably, ROS_g and ROS_p exhibited a consistent seasonal pattern, with maximum values in spring (2.28 ppbv and 0.50 μg m^{-3}, respectively) and minimum values in autumn (1.03 ppbv and 0.17 μg m^{-3}, respectively).

Reference:

Hua, W., Chen, Z., Jie, C., Kondo, Y., Hofzumahaus, A., Takegawa, N., Chang, C., Lu, K., Miyazaki, Y., and Kita, K.: Atmospheric hydrogen peroxide and organic hydroperoxides during PRIDE-PRD'06, China: their concentration, formation mechanism and contribution to secondary aerosols, Atmospheric Chemistry and Physics, 8, 6755-6773, https://doi.org/10.5194/acp-8-6755-2008, 2008.

Huang, W., Zhang, Y., Zhang, Y., Zeng, L., Dong, H., Huo, P., Fang, D., and Schauer, J. J.: Development of an automated sampling-analysis system for simultaneous measurement of reactive oxygen species (ROS) in gas and particle phases: GAC-ROS, Atmospheric environment, 134, 18-26, https://doi.org/10.1016/j.atmosenv.2016.03.038, 2016.

King, L. E. and Weber, R. J.: Development and testing of an online method to measure ambient fine particulate reactive oxygen species (ROS) based on the 2', 7'-dichlorofluorescin (DCFH) assay, Atmospheric Measurement Techniques, 6, 1647-1658, https://doi.org/10.5194/amt-6-1647-2013, 2013.

Kolthoff, I. M. and Medalia, A. I.: The reaction between ferrous iron and peroxides. I. Reaction with hydrogen peroxide in the absence of oxygen, Journal of the American Chemical Society, 71, 3777-3783, https://doi.org/10.1021/ja01179a057, 1949.

Komazaki, Y., Inoue, T., and Tanaka, S.: Automated measurement system for H_2O_2 in the atmosphere by diffusion scrubber sampling and HPLC analysis of Ti (IV)-PAR-H_2O_2 complex, Analyst, 126, 587-593, https://doi.org/10.1039/B008134P, 2001.

Lazrus, A. L., Kok, G. L., Lind, J. A., Gitlin, S. N., Heikes, B. G., and Shetter, R. E.: Automated fluorometric method for hydrogen peroxide in air, Analytical chemistry, 58, 594-597, https://doi.org/10.1021/ac00294a024, 1986.

Liu, Y., Tang, X., Zhang, Z., Li, L., and Chen, J.: Development and Field Testing of an Online Monitoring System for Atmospheric Particle-Bound Reactive Oxygen Species (ROS), Atmosphere, 14, 924, https://doi.org/10.3390/atmos14060924, 2023.

Montesinos, V. N., Sleiman, M., Cohn, S., Litter, M. I., and Destaillats, H.: Detection and quantification of reactive oxygen species (ROS) in indoor air, Talanta, 138, 20-27, https://doi.org/10.1016/j.talanta.2015.02.015, 2015.

Wragg, F. P., Fuller, S. J., Freshwater, R., Green, D. C., Kelly, F. J., and Kalberer, M.: An automated online instrument to quantify aerosol-bound reactive oxygen species (ROS) for ambient measurement and health-relevant aerosol studies, Atmospheric Measurement Techniques, 9, 4891-4900, https://doi.org/10.5194/amt-9-4891-2016, 2016.

Zhou, J., Bruns, E. A., Zotter, P., Stefenelli, G., Prévôt, A. S., Baltensperger, U., El-Haddad, I., and Dommen, J.: Development, characterization and first deployment of an improved online reactive oxygen species analyzer, Atmospheric Measurement Techniques, 11, 65-80, https://doi.org/10.5194/amt-11-65-2018, 2018.